

New effective treatment of the light-front nonvalence contribution in timelike exclusive processes

Chueng-Ryong Ji and Ho-Meoyng Choi

Department of Physics, North Carolina State University, Raleigh, N.C. 27695-8202

(December 2, 2024)

We discuss a necessary nonvalence contribution in timelike exclusive processes. Following a Schwinger-Dyson type of approach, we relate the nonvalence contribution to an ordinary light-front wave function that has been extensively tested in the spacelike exclusive processes. A complicated four-body energy denominator is exactly cancelled in summing the light-front time-ordered amplitudes. Applying our method to $K_{\ell 3}$ and $D^0 \rightarrow K^- \ell^+ \nu_\ell$ where a rather substantial nonvalence contribution is expected, we find not only an improvement in comparing with the experimental data but also a covariance (i.e. frame-independence) of existing light-front constituent quark model.

PACS numbers: 14.40.Aq, 12.39.Ki, 13.10.+q, 13.20.Eb

With the wealth of new and upgraded B-meson factories, exclusive decay processes will be studied intensively. Unlike the leading twist structure functions measured in deep inelastic scattering, such exclusive channels are sensitive to the structure of the hadrons at the amplitude level and to the coherence between the contributions of the various quark currents and multi-parton amplitudes. The central unknown required for reliable calculations of weak decay amplitudes are thus the hadronic matrix elements.

Perhaps, one of the most popular formulations for the analysis of exclusive processes involving hadrons may be provided in the framework of light-front (LF) quantization [1]. In particular, the Drell-Yan-West ($q^+ = q^0 + q^3 = 0$) frame has been extensively used in the calculation of various electroweak form factors and decay processes [2–4]. As an example, only the parton-number-conserving (valence) Fock state contribution is needed in $q^+ = 0$ frame when the “good” component of the current, J^+ or $\mathbf{J}_\perp = (J_x, J_y)$, is used for the spacelike electromagnetic form factor calculation of pseudoscalar mesons. The LF approach may also provide a bridge between the two fundamentally different pictures of hadronic matter, i.e. the constituent quark model (CQM) (or the quark parton model) closely related to the experimental observations and the quantum chromodynamics (QCD) based on a covariant non-abelian quantum field theory. The key of possible connection between the two pictures is the rational energy-momentum dispersion relation (i.e. the square root operator does not appear) that leads to a relatively simple vacuum structure. There is no spontaneous creation of massive fermions in the LF quantized vacuum. Thus, one can immediately obtain a constituent-type pic-

ture, in which all partons in a hadronic state are connected directly to the hadron instead of being simply disconnected excitations (or vacuum fluctuations) in a complicated medium. A possible realization of chiral symmetry breaking in the LF vacuum has also been discussed in the literature [5].

On the other hand, the analysis of timelike exclusive processes has remained as a rather significant challenge in the LF approach. In principle, the $q^+ \neq 0$ frame can be used to compute the timelike processes but then it is inevitable to encounter the particle-number-nonconserving Fock state (or nonvalence) contribution. The main source of difficulty in CQM phenomenology is the lack of information on the non-wave-function vertex (black blob in Fig. 1(a)) in the nonvalence diagram arising from the quark-antiquark pair creation/annihilation. The non-wave-function vertex (black blob) was recently also called the embedded state [6]. This should contrast with the white blob representing the usual LF valence wave function.

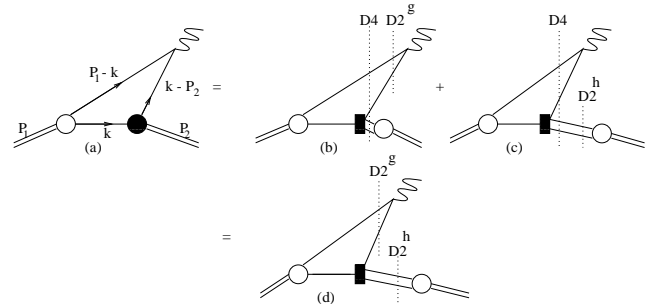


FIG. 1. Effective treatment of the LF nonvalence amplitude.

In principle, there is a systematic program laid out by Brodsky and Hwang [7] to include the particle-number-nonconserving amplitude to take into account the nonvalence contributions. However, the program requires to find all the higher Fock-state wave functions while there has been relatively little progress in computing the basic wave functions of hadrons from first principles. Recently, a method of analytic continuation from the spacelike region has also been suggested to generate necessary information in the timelike region without encountering a direct calculation of the nonvalence contribution [8]. Even though some explicit example has been presented for manifestly covariant theoretical models, this method has not yet been implemented to more realistic phenomenological models.

In this letter, we thus present an alternative way of handling the nonvalence contribution. Our aim of new treatment is to make the program more suitable for the CQM phenomenology specific to the low momentum transfer processes. Incidentally, the light-to-light ($K_{\ell 3}$) and heavy-to-light ($D^0 \rightarrow K^{-\ell^+\nu_\ell}$) decays involving rather low momentum transfers bear a substantial contribution from the nonvalence part and their experimental data are better known than other semileptonic processes with large momentum transfers. Including the nonvalence contribution, our results on $K_{\ell 3}$ and $D^0 \rightarrow K^{-\ell^+\nu_\ell}$ not only show a definite improvement in comparison with experimental data but also exhibit a covariance (i.e frame-independence) of our approach.

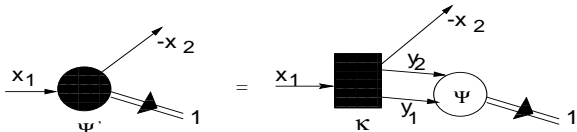


FIG. 2. Non-wave-function vertex(black blob) linked to an ordinary LF wave function(white blob).

To illustrate our method, we first discuss a following link between the non-wave-function vertex (black blob) and the ordinary LF wave function (white blob) as shown in Fig. 2, i.e.,

$$(M^2 - M_0'^2)\Psi'(x_i, \mathbf{k}_{\perp i}) = \int [dy][d^2\mathbf{1}_{\perp}]\mathcal{K}(x_i, \mathbf{k}_{\perp i}; y_j, \mathbf{1}_{\perp j})\Psi(y_j, \mathbf{1}_{\perp j}), \quad (1)$$

where M is the mass of outgoing meson and $M_0'^2 = (m_1^2 + \mathbf{k}_{\perp 1}^2)/x_1 - (m_2^2 + \mathbf{k}_{\perp 2}^2)/(-x_2)$ with $x_1 = 1 - x_2 > 1$ due to the kinematics of the non-wave-function vertex. This link can be made following the idea of iteration in a Schwinger-Dyson (SD) type of approach presented in Ref. [9]. As shown in the literature [6], the LF energy integration reveals an explicit correspondence between the sum of LF time-ordered amplitudes and the original covariant amplitude. We thus iterated the covariant Bethe-Salpeter (BS) amplitude (See Eq.(3) below) and performed the LF energy (k^-) integration to pin down the corresponding LF time-ordered diagrams before and after the iteration. We did not assume any particular form of the kernel but left it general at a starting point. This procedure led us to figure out the correspondence between the non-wave-function vertex (black blob) and the convolution of the kernel with the ordinary LF wave function (white blob) and realize that Eq.(1) naturally arises. This equation essentially takes the same form as the LF bound state equation (similar to the LF projection of Bethe-Salpeter equation) except the difference in kinematics(e.g. $-x_2 > 0$ for the non-wave-function vertex). Incidentally, Einhorn [10] also discussed the extension of the LF BS amplitude in 1+1 QCD to a non-wave-function vertex similar to what we obtained in this work.

In the above procedure, we also find that the four-body

energy denominator D_4 is exactly cancelled in the sum of LF time-ordered amplitudes as shown in Figs. 1(b) and 1(c), i.e., $1/D_4 D_2^g + 1/D_4 D_2^h = 1/D_2^g D_2^h$. We thus obtain the amplitude identical to the nonvalence contribution in terms of ordinary LF wave functions of gauge boson(W) and hadron (white blob) as drawn in Fig.1(d). This method, however, requires to have some relevant operator depicted as the black square(\mathcal{K}) in Fig. 2(See also Fig.1(d)), that is in general dependent on the involved momenta connecting one-body to three-body sector. We now present some details of kinematics in the semileptonic decay processes to discuss a reasoning of how we handle the nonvalence contribution involving the momentum-dependent \mathcal{K} for relatively small momentum transfer processes such as $K_{\ell 3}$ and $D \rightarrow K\ell\nu$.

The semileptonic decay of $Q_1\bar{q}$ bound state with four-momentum P_1^μ and mass M_1 into another $Q_2\bar{q}$ bound state with P_2^μ and M_2 is governed by the weak current, viz.,

$$J^\mu(0) = \langle P_2 | \bar{Q}_2 \gamma^\mu Q_1 | P_1 \rangle = f_+(q^2)(P_1 + P_2)^\mu + f_-(q^2)q^\mu, \quad (2)$$

where $q^\mu = (P_1 - P_2)^\mu$ is the four-momentum transfer to the lepton pair ($\ell\nu$) and $m_\ell^2 \leq q^2 \leq (M_1 - M_2)^2$. The covariant three-point BS amplitude of the total current $J^\mu(0)$ in Eq. (2) may be given by

$$J^\mu(0) = iN_c \int \frac{d^4k}{(2\pi)^4} \frac{H_{1[2]}^{\text{cov}} H_2^{\text{cov}} S^\mu}{(p_1^2 - m_1^2 + i\epsilon)(p_2^2 - m_2^2 + i\epsilon)} \times \frac{1}{(p_q^2 - m_q^2 + i\epsilon)}, \quad (3)$$

where N_c is the color factor, $H_{1[2]}^{\text{cov}}$ is the covariant initial[final] state meson-quark vertex function, and $S^\mu = \text{Tr}[\gamma_5(\not{p}_1 + m_1)\gamma^\mu(\not{p}_2 + m_2)\gamma_5(-\not{p}_q + m_q)]$. The quark momentum variables are given by $p_1 = P_1 - k$, $p_2 = P_2 - k$, and $p_q = k$. Performing the k^- pole integration as discussed above, we obtain the LF currents, J_V^μ and J_{NV}^μ corresponding to the usual LF valence diagram and the nonvalence diagram shown in Fig. 1(a), respectively. In purely longitudinal momentum frame where $q^+ > 0$ and $\mathbf{P}_{1\perp} = \mathbf{P}_{2\perp} = 0$, the momentum transfer $q^2 = q^+q^-$ can be written in terms of the momentum fraction $\alpha = P_2^+/P_1^+ = 1 - q^+/P_1^+$ as $q^2 = (1 - \alpha)(M_1^2 - M_2^2/\alpha)$. With the iteration procedure in this frame, the results for the “+”-component of the current J^μ are given by

$$J_V^+ = \frac{N_c}{16\pi^3} \int_0^\alpha dx \int d^2\mathbf{k}_\perp \frac{\Psi_i(x, \mathbf{k}_\perp) S_V^+ \Psi_f(x', \mathbf{k}_\perp)}{x(1-x)(1-x')}, \quad (4)$$

and

$$J_{NV}^+ = \frac{N_c}{16\pi^3} \int_\alpha^1 dx \int d^2\mathbf{k}_\perp \frac{\Psi_i(x, \mathbf{k}_\perp) S_{NV}^+}{x(1-x)(x'-1)} \left(\frac{1}{\alpha D_2^g} \right) \times \int \frac{dy}{y(1-y)} \int d^2\mathbf{1}_\perp \mathcal{K}(x, \mathbf{k}_\perp; y, \mathbf{1}_\perp) \Psi_f(y, \mathbf{1}_\perp), \quad (5)$$

where $x = k^+/P_1^+$, $x' = x/\alpha$, $D_2^g = q^- - p_1^- - (-p_2^-)$ with $-p_2^- > 0$ and $\Psi_{i[f]}(x, \mathbf{k}_\perp) = h_{1[2]}^{LF}/(M_{1[2]}^2 - M_{01[02]}^2)$ with $M_{01}^2[M_{02}^2] = m_{1\perp}^2/(1-x) + m_{\bar{q}\perp}^2/x[m_{2\perp}^2/(1-x') + m_{\bar{q}\perp}^2/x']$ (the invariant mass of the initial[final] state) and $m_{i\perp}^2 = m_i^2 + \mathbf{k}_\perp^2$. Here, Eq. (1)(SD type equation) was folded in the derivation of Eq. (5) by the iteration procedure. While the relevant operator \mathcal{K} is in general dependent on all internal momenta $(x, \mathbf{k}_\perp, y, \mathbf{l}_\perp)$, a sort of average on \mathcal{K} over y and \mathbf{l}_\perp in Eq.(5) which we define as $G_{P_1 P_2} \equiv \int [dy][d^2\mathbf{l}_\perp] \mathcal{K}(x, \mathbf{k}_\perp; y, \mathbf{l}_\perp) \Psi_f(y, \mathbf{l}_\perp)$ is dependent only on x and \mathbf{k}_\perp . Now, the range of the momentum fraction x depends on the external momenta for the embedded states. As shown in Eq.(5), the lower bound of x for the kernel in the nonvalence contribution is given by α which has the value $\alpha = M_2/M_1$ at the maximum q^2 . As the mass difference between the primary and secondary mesons gets smaller, not only the range of q^2 is reduced but also α gets closer to 1. In Ademollo-Gatto's SU(3) limit [11], the q^2 range of the nonvalence contribution shrinks to zero and α becomes precisely 1. Furthermore, the initial wavefunction $\Psi_i(x, \mathbf{k}_\perp)$ plays the role of an weighting factor in the nonvalence contribution and enfeeble the contribution from the region of x near 1. Thus, smaller the difference between M_1 and M_2 is, narrower the effective x region gets for the nonvalence contribution. Similarly, the region of the transverse momentum \mathbf{k}_\perp is also limited only up to the scale of hadron size due to the same weighting factor $\Psi_i(x, \mathbf{k}_\perp)$. In this work, we thus approximate $G_{P_1 P_2}$ as a constant and examine the validity of this approximation by checking the frame independence of our numerical results.

In Eqs.(4) and (5), the trace terms $S_V^+(p_{\bar{q}}^- = k_{\text{on}}^-) = (4P_1^+/x')\{\mathbf{k}_\perp^2 + [xm_1 + (1-x)m_{\bar{q}}][x'm_2 + (1-x')m_{\bar{q}}]\}$ and $S_{NV}^+ = S_V^+(p_i^- = p_{\text{ion}}^-) + 4p_{1\text{on}}^+ p_{2\text{on}}^+(p_{\bar{q}}^- - p_{\text{ion}}^-)$ correspond to the product of initial and final LF spin-orbit wave functions that are uniquely determined by a generalized off-energy-shell Melosh transformation. Here, the subscript (on) means on-mass-shell and the instantaneous part of nonvalence diagram corresponds to $S_{NV}^+ - S_V^+(p_i^- = p_{\text{ion}}^-)$. While the LF vertex function $h_{1[2]}^{LF}$ formally stems from $H_{1[2]}^{\text{cov}}$, practical informations on the radial wave function $\Psi_{i[f]}(x, \mathbf{k}_\perp)$ (consequently $h_{1[2]}^{LF}$) can be obtained by LF CQM. The details of our variational procedure to determine both mass spectra and wave functions of pseudoscalar mesons were recently documented in Refs. [3,4] along with an extensive test of the model in the spacelike exclusive processes. The same model is used in this work.

For the check of frame-independence, we also compute the "+" component of the current J_D^μ in the Drell-Yan-West ($q^+ = 0$) frame where only valence contribution exists. Since the form factor $f_+(q^2)$ obtained from J_D^+ in $q^+ = 0$ frame is immune to the zero-mode contribution [4,7,12,13], the comparison of $f_+(q^2)$ in the two completely different frames (i.e. $q^+ = 0$ and $q^+ \neq 0$) would reveal the validity of existing model with respect to a covariance. The comparison of $f_-(q^2)$, however, can-

not give a meaningful test of covariance because of the zero-mode complication as noted in Ref. [13]. Indeed, the difference between the two ($q^+ = 0$ and $q^+ \neq 0$) results of $f_-(q^2)$ amounts to the zero-mode contribution [12].

In our numerical calculation for the processes of $K_{\ell 3}$ and $D^0 \rightarrow K^-\ell^+\nu$ decays, we use the linear potential parameters presented in Ref. [4]. In Fig. 3, we show the weak form factors $f_+(q^2)$ and $f_0(q^2) = f_+(q^2) + q^2 f_-(q^2)/(M_1^2 - M_2^2)$ for $K_{\ell 3}^0$ decays. The thick solid lines are our analytic solutions obtained from the $q^+ = 0$ frame; note here again that the lower thick solid line (f_0) in Fig. 3 is only the partial result without including the zero-mode contribution while the upper thick solid line (f_+ immune to the zero-mode) is the full result. The thin solid lines are the full results of our effective calculations with a constant ($G_{K\pi} = 3.95$) fixed by the normalization of f_+ at $q^2 = 0$ limit. For comparison, we also show only the valence contributions(dotted lines) in $q^+ \neq 0$ frame. As expected, a clearly distinguishable nonvalence contribution is found. Following the popular linear parametrization [14], we plot the results of our effective solutions(thin solid lines) using $f_i(q^2) = f_i(q^2 = m_\ell^2)(1 + \lambda_i q^2/M_{\pi^+}^2)$ ($i = +, 0$). In comparison with the data, the same normalization as the data $f_+(0) = 1$ [15] was used in Fig. 3. Our effective solution(upper thin solid line) is not only in a good agreement with the data [15] but also almost identical to that in $q^+ = 0$ frame(upper thick solid line) indicating the frame-independence of our model. Note also that the difference in $f_0(q^2)$ between $q^+ \neq 0$ (lower thin solid line) and $q^+ = 0$ (lower thick solid line) frames amounts to the zero-mode contribution [12].

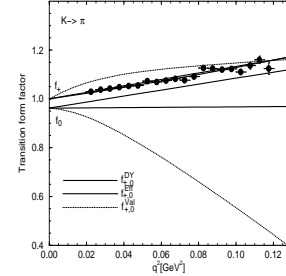


FIG. 3. The weak form factors for $K_{\ell 3}^0$ compared with the experimental data [15].

In comparison with experimental data, we summarized our results of several experimental observables in Table I; i.e. the actual value of $f_+(0)$, the slopes $\lambda_+ [\lambda_0]$ of $f_+(q^2)$ [$f_0(q^2)$] at $q^2 = 0$, $\xi_A = f_-(0)/f_+(0)$, and the decay rates $\Gamma(K_{e3}^0)$ and $\Gamma(K_{\mu 3}^0)$. In the second column of Table I, our full results including nonvalence contributions are presented along with the valence contributions in the square brackets. In the third column of Table I, the results in $q^+ = 0$ frame are presented with[without] the instantaneous part. As one can see in Table I, adding the nonvalence contributions clearly improves the results of λ_0 , i.e.

our full result of $\lambda_0 = 0.025$ is in an excellent agreement with the data, $\lambda_0^{\text{Exp.}} = 0.025 \pm 0.006$. The results of ξ_A and $\Gamma(K_{\mu 3}^0)$ seem to be also improved by our full effective calculations including the nonvalence contributions.

In Figs. 4(a,b), we show the weak form factors for $D^0 \rightarrow K^- \ell^+ \nu$ decays and compare with the experimental data [14](full dot) with an error bar at $Q^2 = 0$ as well as the lattice QCD results [16](circle and square) and [17](cross). All the line assignments are same as in Fig. 3. In Fig. 4(a), the thin solid line of our full result in $q^+ \neq 0$ is not visible because it exactly coincides with the thick solid line of the result in $q^+ = 0$ confirming the frame-independence of our calculations. Our value of $f_+(0) = 0.736$ is also within the error bar of the data [14], $f_+^{\text{Exp.}}(0) = 0.7 \pm 0.1$. In Fig. 4(b), the difference between the thin and thick solid lines is the measure of the zero-mode contribution to $f_0(q^2)$ in $q^+ = 0$ frame [12]. The form factors obtained from our effective calculations ($G_{DK} = 3.5$) are also plotted with the usual parametrization of pole dominance model, i.e. $f_{+(0)}(q^2) = f_{+(0)}(0)/(1 - q^2/M_{1-(0+)}^2)$. Our pole masses turn out to be $M_{1-} = 2.16$ GeV and $M_{0+} = 2.79$ GeV, respectively, and we note that $M_{1-} = 2.16$ GeV is in a good agreement with the mass of D_s^* , i.e. 2.1 GeV. Using CKM matrix element $|V_{cs}| = 1.04 \pm 0.16$ [14], our branching ratios $\text{Br}(D_{e3}^0) = 3.73 \pm 1.24$ and $\text{Br}(D_{\mu 3}^0) = 3.60 \pm 1.19$ are also comparable with the experimental data 3.64 ± 0.18 and 3.22 ± 0.17 [14], respectively.

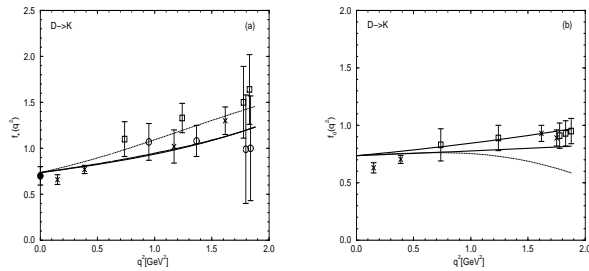


FIG. 4. The weak form factors for $D \rightarrow K$ transition.

In summary, we presented an effective treatment of the LF nonvalence contributions crucial in the timelike exclusive processes. Using a SD-type approach and summing the LF time-ordered amplitudes, we obtained the nonvalence contributions in terms of ordinary LF wavefunctions of gauge boson and hadron that have been extensively tested in the spacelike exclusive processes. Including the nonvalence contribution, our results show a definite improvement in comparison with experimental data on $K_{\ell 3}$ and $D^0 \rightarrow K^- \ell^+ \nu_\ell$ decays. The frame-independence of our results also indicate that a constant $G_{P_1 P_2}$ is an approximation appropriate to the small momentum transfer processes. Applications to the heavy-to-light decay processes involving large momentum transfers would require an improvement on this approximation

perhaps guided by the perturbative QCD approach. Consideration along this line is underway.

This work was supported by the US DOE under contracts DE-FG02-96ER40947. The North Carolina Supercomputing Center and the National Energy Research Scientific Computer Center are also acknowledged for the grant of supercomputer time.

-
- [1] S. J. Brodsky, H.-C. Pauli, and S. S. Pinsky, Phys. Rept. **301**, 299(1998).
 - [2] W. Jaus, Phys. Rev. D **44**, 2851 (1991).
 - [3] H.-M. Choi and C.-R. Ji, Phys. Rev. D **59**, 074015 (1999).
 - [4] H.-M. Choi and C.-R. Ji, Phys. Lett. B **460**, 461 (1999); Phys. Rev. D **59**, 034001 (1999).
 - [5] L. Susskind and M. Burkardt, pp. 5 in Proceedings of the 4th International Workshop on Light-Front Quantization and Non-Perturbative Dynamics edited by S. D. Glazek (1994); K. G. Wilson and D. G. Rebertson, pp. 15 in the same proceedings.
 - [6] B. L. G. Bakker and C.-R. Ji, Phys. Rev. D **62**, 074014 (2000).
 - [7] S. J. Brodsky and D. S. Hwang, Nucl. Phys. B **543**, 239 (1998).
 - [8] H.-M. Choi and C.-R. Ji, to be published in Nucl. Phys. A, hep-ph/9906225.
 - [9] S.J. Brodsky, C.-R. Ji and M. Sawicki, Phys. Rev. D **32**, 1530 (1985); More recent formal discussion can be found in J.H.O. Sales, et. al., Phys. Rev. C **61**, 044003 (2000).
 - [10] M.B.Einhorn, Phys. Rev. D **14**, 3451 (1976).
 - [11] M. Ademollo and R. Gatto, Phys. Rev. Lett. **13**, 264 (1964).
 - [12] S. J. Chang, R. G. Root, and T. M. Yan, Phys. Rev. D **7**, 1133 (1973); M. Burkardt, Nucl. Phys. A **504**, 762 (1989); H.-M. Choi and C.-R. Ji, Phys. Rev. D **58**, 071901 (1998).
 - [13] W. Jaus, Phys. Rev. D **60**, 054026 (1999).
 - [14] Particle Data Group, Eur. Phys. J. C **3**, 1(1998).
 - [15] Apostolakis A et al., Phys. Lett. B **473**, 186 (2000).
 - [16] C. W. Bernard et al., Phys. Rev. D **43**, 2140 (1991).
 - [17] K. C. Bowler et al., Phys. Rev. D **51**, 4905 (1995).

TABLE I. Model predictions for the parameters of $K_{\ell 3}^0$ decays. The decay width is in units of 10^6 s^{-1} . The used CKM matrix is $|V_{us}| = 0.2196 \pm 0.0023$ [14].

	Effective	$q^+ = 0$	Experiment
$f_+(0)$	0.962 [0.962]	0.962 [0.962]	
λ_+	0.026 [0.083]	0.026 [0.026]	$0.0288 \pm 0.0015 [K_{e3}^0]$
λ_0	0.025 [-0.017]	0.001 [-0.009]	$0.025 \pm 0.006 [K_{\mu 3}^0]$
ξ_A	-0.013 [-1.10]	-0.29[-0.41]	$-0.11 \pm 0.09 [K_{\mu 3}^0]$
$\Gamma(K_{e3}^0)$	7.3 ± 0.15	7.3 ± 0.15	7.5 ± 0.08
$\Gamma(K_{\mu 3}^0)$	4.92 ± 0.10	4.66 ± 0.10	5.25 ± 0.07